Navier-Stokes Simulation of Unsteady Rotor-Airframe Interaction with Momentum Source Method

Young-Hwa Kim* and Seung-O Park**
Department of Aerospace Engineering, KAIST, Daejeon, Korea

Abstract

To numerically simulate aerodynamics of rotor-airframe interaction in a rigorous manner, we need to solve the Navier-Stokes system for a rotor-airframe combination as a whole. This often imposes a serious computational burden since rotating blades and a stationary body have to be simultaneously dealt with. An efficient alternative is to adopt a momentum source method in which the action of rotor is approximated as momentum source over a rotor disc plane in a stationary computational domain. This makes the simulation much simpler. For unsteady simulation, the instantaneous momentum sources are assigned only to a portion of disk plane corresponding to blade passage. The momentum source is obtained by using blade element theory with dynamic inflow model. Computations are carried out for the simple rotor-airframe model (the Georgia Tech model) and the results of the simulation are compared with those of the full Navier-Stokes simulation with moving mesh system for rotor and with experimental data. It is shown that the present simulation yields results as good as those of the full Navier-Stokes simulation.

Key words : Momentum Source Method, Rotor-Airframe Interaction, Unsteady Navier-Stokes Simulation, Blade Element Theory, Moving Mesh

Introduction

The flow field around a rotor is very complex due to the unsteadiness of the complex rotor wake and mutual aerodynamic interferences. The strength of interaction depends on the relative position of the rotor and the body, and on flight conditions. This highly coupled aerodynamic interaction plays an important role in determining aerodynamic characteristics and performance of a rotorcraft.

Many computational methods have been developed to predict rotor-airframe interaction. Rotorcraft Wake Analysis and a source/vortex fuselage panel method have been coupled to predict the interaction between the two components [1]. This approach was one of many earlier attempts to account for rotor-airframe interaction [2, 3]. Following these attempts, Euler or Reynolds-Averaged Navier-Stokes (RANS) equations have been used in the analysis of rotor-airframe interactions. The analysis of rotor-airframe interaction requires an unsteady three-dimensional solver which can model the actual unsteady motion of the rotor. Generally, both structured and unstructured mesh systems are used for solving unsteady Euler or RANS equations. Some applications of structured grid for complex geometries have been successfully made using overset or Chimera grid methodology [4, 5].

* Student Researcher
** Professor
E-mail : sopark@kaist.ac.kr Tel : +82-42-350-3713 Fax : +82-42-350-3710

Unstructured grid methods are easier to adapt to complex configurations. Recently, unstructured three-dimensional Euler solver was developed using a sliding mesh algorithm, in which the computational domain is divided into a moving zone rotating with the blades and a stationary zone for airframe [6].

As is well known, computational burden becomes heavy when RANS simulations is adopted either for overset or sliding mesh scheme since rotating blades and a stationary body must be simultaneously dealt with in a single computational domain. One approach to mitigate this is to consider only the time-averaged behavior of the rotor, leading to the concept of an actuator disk instead of moving mesh for rotating blades. Two different models exist : pressure disk model and momentum source model. The pressure disk rotor model approximates a rotor in a time-averaged manner using inflow and outflow boundary conditions at the surface of the disk [7]. This model uses a modified actuator disk that allows a pressure jump varying with radius and azimuth across the disk. Another is the momentum source method in which the action of rotor is approximated as a momentum source applied in the disk plane[8-13]. For example, this method was utilized to analyze mutual aerodynamic interactions between multiple rotors and airframes using FLUENT [14].

For the time-averaged momentum source method developed by Rajagopalan[8-13], the time-averaged momentum sources are applied to the entire disk plane. The momentum sources are not known at the start of the calculation, but computed as part of the solution via iteration. The local angle of attack and velocity at each blade element are obtained from the computed velocity field. The magnitudes of the momentum sources are determined by the blade element theory using this local angle of attack and velocity. Then, the momentum sources are updated to the flow field. Updating the momentum sources and computing the flow field are iterated until the solution is converged. Through this method, the time-averaged rotor-airframe interaction can be predicted. Thus, this method is not adequate to simulate unsteady behaviors of rotor-airframe interaction. For unsteady simulation, the momentum source needs be estimated as the rotor rotates and therefore the momentum source is present only for the region of blade passage and changes along the azimuth. To determine the momentum source, induced velocity field toward rotor blade should be known. The calculation of induced velocity field, however, is somewhat complicated. For efficient induced velocity prediction, various inflow models have been developed. Linear inflow models such as Coleman, Drees and Payne assume that the induced velocities of a rotor disk are linearly distributed by Fourier first harmonic variations [15]. These models are simple and easy to apply. However, unsteady aerodynamics of rotor can hardly be solved by using these models since these models cannot simulate time-varying dynamic inflow behavior. Dynamic inflow models such as Pitt-Peters and Peters-He models have been developed to resolve this situation [16, 17].

In the present study, we intend to apply dynamic inflow models of Pitt-Peters and Peters-He to estimate 'unsteady' momentum sources for the unsteady Navier-Stokes (NS) simulation. Airload of each blade element is calculated by using aerodynamic coefficients of 2D airfoil look-up table made from a two dimensional NS simulation. As we simply adopt inflow models to determine induced velocities, the influence of airframe is not reflected. Momentum source data so obtained corresponding to each blade passage is then fed to a stationary NS computational domain which encloses the airframe. The results of the simulation are compared with those from the solution obtained by solving the NS system for an entire domain with moving mesh system employed. The present NS computations are carried out for the simplified rotor-airframe model (the Georgia Tech configuration) using STAR-CD.

Numerical method

As mentioned earlier, two different simulations are carried out. : (1) Unsteady NS simulation for an entire domain with moving mesh system and (2) Unsteady NS simulation for a stationary domain with unsteady momentum source. The moving mesh method is provided by the commercial code STAR-CD[20].

Simulations for unsteady momentum source method are carried out in two steps: (1) Computation of unsteady airload of rotor by the blade element theory coupled with dynamic inflow model. (2) Unsteady flow field computation around the airframe in a stationary computational domain where a rotor-disk plane is embedded to reflect rotor aerodynamics by means of momentum source. As mentioned already, computations and grid generations have been performed by using STAR-CD. A conceptual flow chart for the present computation using STAR-CD is given in Fig. 1. The computation is carried out against the Georgia Tech Rotor-airframe model (Fig. 2).

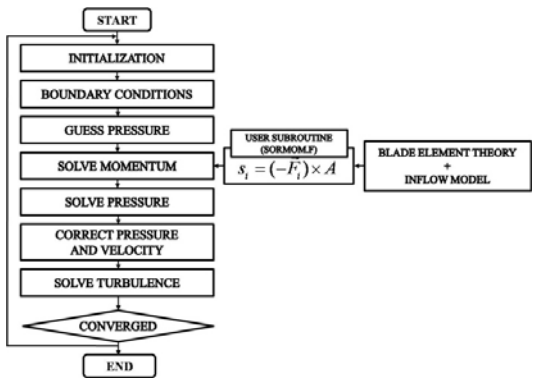

Fig. 1. The flowchart of Momentum source method using STAR-CD

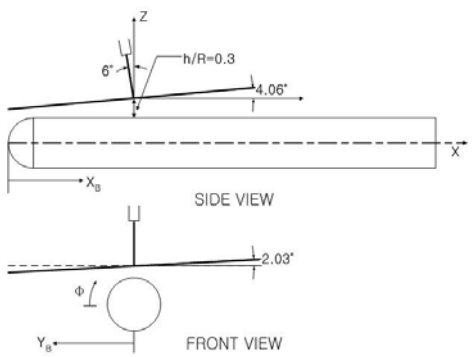

Fig. 2. Georgia Tech rotor-airframe schematic

2.1 Blade Element Theory

The blade element theory can estimate the radial and azimuthal distributions of airloads for each blade element. It assumes that each blade element acts as a 2-D airfoil to produce aerodynamic forces (lift and drag). Rotor performance such as thrust and moment can be obtained by integrating the resultant 2-D airloads at each blade element employed. To account for 3-D effects, tip and hub loss correction such as Prandtl's tip loss model or other empirical factors need be applied [15]. As is well known, Pitt-Peters model should be accompanied by a tip loss model while Peters-He model does not requires additional tip loss model. In the present simulation, we employ Prandtl's tip loss model.

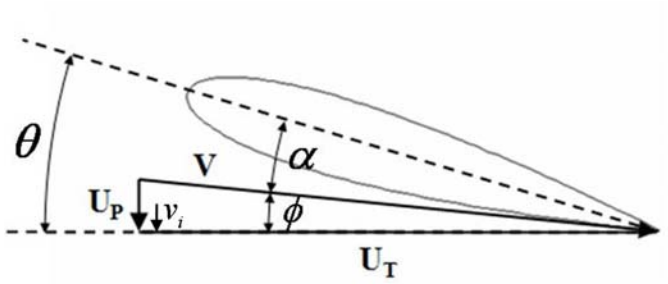

Fig. 3. Aerodynamic environment at a blade element

To properly obtain unsteady airloads for the blades, it is necessary to determine the magnitude and direction of local velocity at each blade element. Fig. 3 shows the aerodynamic environment for a blade element at a given set of flight conditions. The resultant velocity toward a blade element with pitch angle θ at the blade element is decomposed into the perpendicular component U_P and the tangential component U_T. As can be found in many references, for example Leishman [15] among others, calculation of U_P and U_T requires various data : freestream velocity V_∞, angular velocity Ω, induced velocity v_i, azimuth angle ψ, pitch angle θ, flapping angle β, angle of attack of the rotor plane α_r. U_P and U_T are given by :

$$U_T = \Omega r + V_\infty \cos\alpha_r \sin\psi \tag{1}$$
$$U_P = V_\infty \sin\alpha_r + v_i + r\dot{\beta} + V_\infty \beta \cos\alpha_r \cos\psi$$

Since the geometric variables α_r and β are given, the induced velocity v_i needs be computed to determine U_P and U_T, which is done by using dynamic inflow models. We adopt two different dynamic inflow models to determine the induced velocity : Pitt-Peters model [16] and Peters-He model [17]. The resultant velocity V and the angle of attack α for each blade element is computed by using U_P and U_T. With this information, we then obtain the aerodynamic coefficients for each blade element from look-up table. In the present work, the look-up table was made from a two dimensional NS simulation using STAR-CD. The momentum source is then computed as described below.

2.2 Flow Field Computation

The governing equations to be solved are the 3-D NS equations with momentum source term added in the momentum equation.

$$\frac{\partial \rho}{\partial t} + \frac{\partial}{\partial x_j}(\rho u_j) = 0 \tag{2}$$

$$\frac{\partial (\rho u_i)}{\partial t} + \frac{\partial}{\partial x_j}(\rho u_j u_i - \tau_{ij}) = -\frac{\partial p}{\partial x_i} + s_i \tag{3}$$

where τ_{ij} the stress tensor and s_i the instantaneous momentum source per unit volume in the i direction. To obtain the momentum source components, the lift and drag forces for each discretized blade segment have to be calculated first. The aerodynamic coefficients C_l and C_d are obtained by the blade element theory coupled with dynamic inflow model as explained in 2.1. Then, the lift and drag forces experienced by the blade element can be computed as

$$L = \frac{1}{2}\rho V^2 C_l c dr \tag{4}$$
$$D = \frac{1}{2}\rho V^2 C_d c dr$$

where c is the blade chord, and dr is the spanwise width of the blade element. These lift and drag forces are converted to the normal force F_n and the tangential force F_t to the disk plane.

$$F_n = L\cos\phi - D\sin\phi \tag{5}$$
$$F_t = L\sin\phi + D\cos\phi$$

where φ is the inflow angle (Fig. 3) given by

$$\phi = \tan^{-1}(-\frac{U_T}{U_P}) \tag{6}$$

These forces are then converted to Cartesian component force vector $\vec{F}_i$ by

$$\vec{F}_i = \begin{pmatrix} \cos\alpha_r & -\sin\alpha_r & 0 \\ \sin\alpha_r & \cos\alpha_r & 0 \\ 0 & 0 & 1 \end{pmatrix} \begin{pmatrix} F_t \sin\psi \\ F_n \\ F_t \cos\psi \end{pmatrix} \tag{7}$$

where α_r is the angle of attack of the rotor disk plane and ψ the azimuth angle. Evidently, $-\vec{F}_i$ is the force vector acting on the fluid which must be the momentum source for the blade element. For unsteady computation, the momentum sources are applied only at the location where the blades are passing. Fig. 4 illustrates the portion of disk plane with non-zero momentum source at one instance. Since this $-\vec{F}_i$ needs to be assigned to computational cells covering the area of blade element, we assume a uniform chordwise distribution to a very first approximation. Then the momentum source for each grid cell can be estimated as

$$S_i = A(-\vec{F}_i) \tag{8}$$

Where

$$A = \frac{A_{disk\,cell}}{A_{blade\,element}} \tag{9}$$

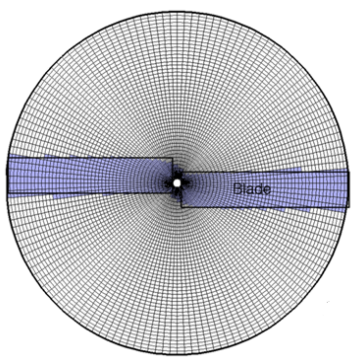

Fig. 4. Location of unsteady momentum source corresponding

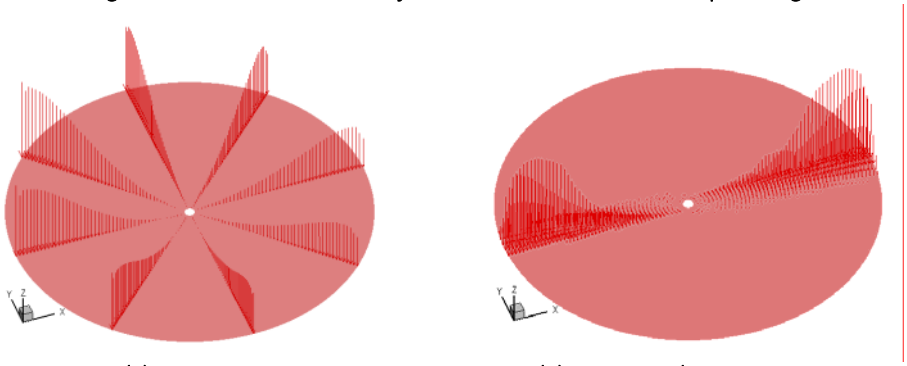

(a) Steady (b) Unsteady (Azimuth=0deg)

Fig. 5. Comparison of the different source distribution between steady and unsteady computation

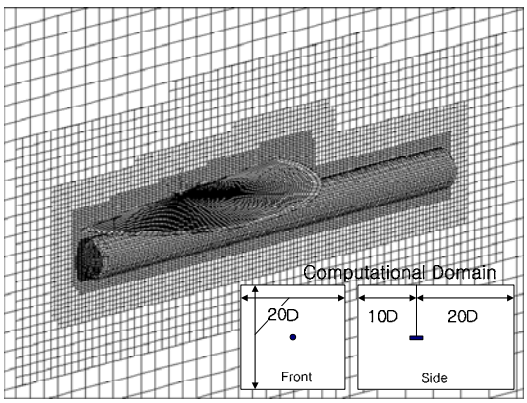

Fig. 6. Computational mesh for unsteady momentum method

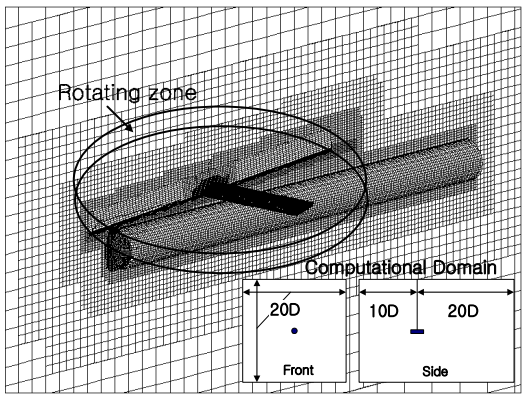

Fig. 7. Computational mesh for moving mesh method

Table 1. No. of Grid and CPU time using 1 processor

Method	Rotor	Total No. of Grid	CPU Time per 1 Rev.
Unsteady Momenum Source	12,200 hexahedral disk cells	800,000 cells	47000sec
Moving Mesh	800,000 moving cells	1500,000 cells	125000sec

For comparison purpose, we compare the present unsteady momentum source distribution and the time averaged momentum source for the entire disk plane in Fig. 5.

Fig. 6 illustrates the grid system and the computational domain for the present momentum source method. The grid contains about 800,000 unstructured cells. The rotor is replaced as hexahedral disk cells. Fig. 7 illustrates the grid system and the computational domain for a moving mesh computation. The computational domain is divided into a rotating zone with the blades and a stationary zone. The grid for moving mesh computation contains about 800,000 cells in the rotating zone and about 700,000 in the stationary zone. The grid system around the airframe is about same for both methods. For the computation with moving mesh, moving mesh grid generation can become laborious as the moving mesh and the stationary mesh should be properly arranged to ensure good results. The rotor proceeds 0.5 degrees for each time step. It requires approximately 13 hours for the unsteady momentum source method and 35 hours for the moving mesh method to rotate one revolution using 1 processor (Table 1).

Time integration is done using the Crank-Nicholson second order scheme and spatial discretization is done using the second order MARS(Monotone Advection and Reconstruction Scheme[20]). The k-ε high Reynolds model with the wall function is used. At the inlet of the computational domain, the flow is considered to be uniform. At the far-field boundary, the pressure is fixed to the freestream value. On the solid surface of the blades and the airframe, the no slip condition is applied.

Results

As mentioned already, the present computation has been performed for a simple configuration(Fig. 2) extensively tested in the Georgia Institute of Technology [18, 19]. This model consists of a cylindrical airframe and two untwisted blades made of NACA0015 airfoil. The freestream conditions for the present work are : Blade tip Mach number=0.295, Advance ratio=0.1.

Fig. 8 shows the blade loading at the azimuth angle of 90deg. The results of the blade element theory using Pitt-Peters model and Peters-He model are compared with the results of NS simulation for a rotor in moving mesh method. We see that the Peters-He model provides a better prediction than the Pitt-Peters model which assumes linear distribution of induced velocity along the radius. From this finding, we use Peters-he model in later computations.

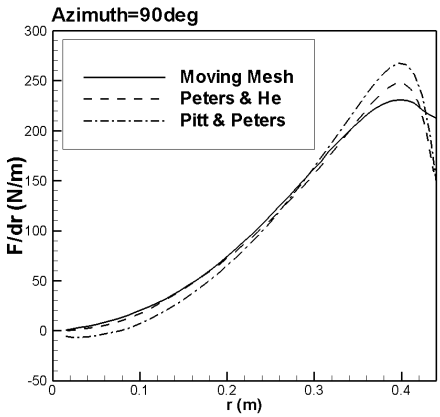

Fig. 8. Blade load distributions along the radius

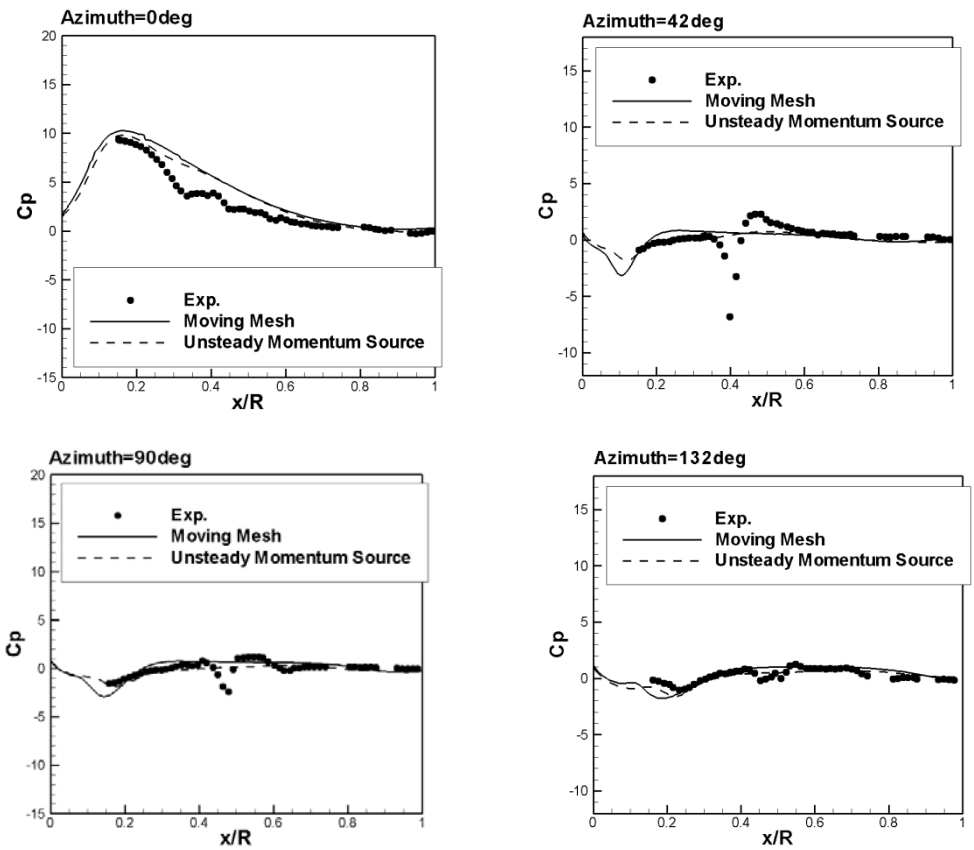

Fig. 9. Instantaneous surface pressure distribution on the top of the airfarme

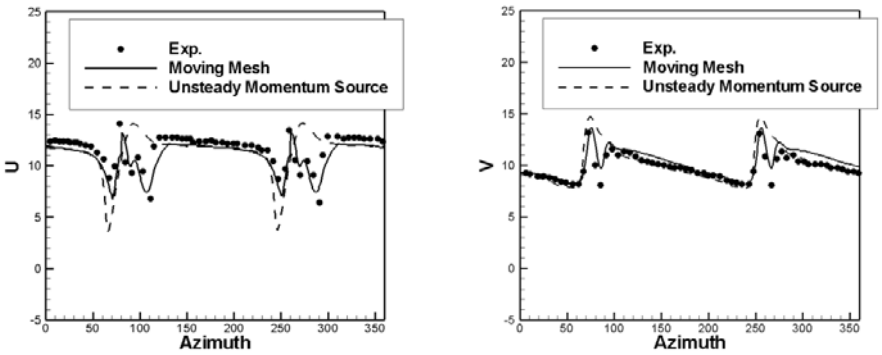

Fig. 10. Azimuth-resolved velocity at fixed point located at r/R=0.667 and 67.5 degree along azimuth line

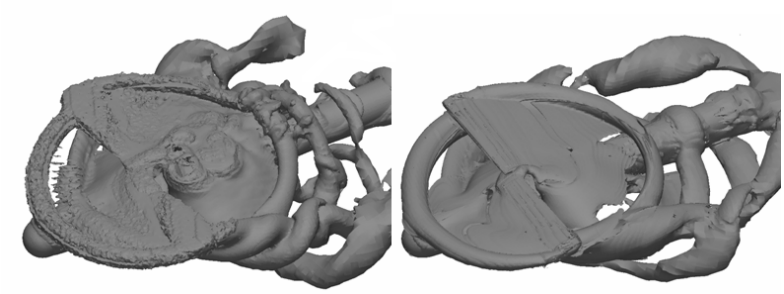

(a) Momentum source method (b) Moving mesh method

Fig. 11. Instantaneous iso-vorticity surface

Fig. 9 compares surface pressure distributions along the top of the airframe at four different blade azimuth angles together with the results from the NS simulation (with moving mesh) and with the experimental data. We see that the present results are in good agreement with those of NS simulation. However, the pressure peak present in the experimental data at some azimuth angles are not predicted properly by these two numerical methods. This pressure peak might have been caused by the tip vortex core impingement [6]. We tried a moving mesh NS simulation with much finer grid system. However, the results remained pretty much the same. We thus imagine that we need a better method to simulate tip vortex flow well.

Fig. 10 compares azimuth-resolved velocity components at the fixed point which is at 12.7mm below the rotor plane, the azimuth angle of 67.5 degree, and r/R=0.667. Downward velocity is positive. The overall velocities are in good agreement with the experimental data. The sharp peaks at 67.5 and 247.5 degree due to blade passage are predicted properly for both methods. However, velocity variation after these sharp peak was adequately simulated for unsteady momentum source method. Fig. 11 shows the instantaneous iso-vorticity surface for both methods. We see that the vortical structures from these two methods are similar each other.

Conclusion

In the present study, an unsteady momentum source method is employed to simulate unsteady rotor-airframe interaction. We adopt the blade element theory coupled with Peters-He inflow model to provide unsteady momentum source in the Navier-Stokes simulation. The Navier-Stokes simulation with moving mesh was also performed to compare the results with those of the unsteady momentum source method. The methods were applied to the simple rotor-airframe configuration tested at Georgia Tech.

Computational time for the present unsteady momentum source method is about 1/3 of the computational time required for the moving mesh computation. Even though there are some discrepancies in the details of the predicted data, the results of the present unsteady momentum source method are in good agreement in an overall sense with the experimental data as can be seen from the pressure distribution curves and the vortical structures.

Acknowledgments

Authors are gratefully acknowledging the financial support by Agency for Defense Development and by UTRC (Unmanned technology Research Center), Korea Advanced Institute of Science and Technology.

References

1. Landgrebe, A. J., Moffitt, R. C., and Clark, D. R., "Aerodynamic Technology for Advanced Rotorcraft, Parts Ⅰ and Ⅱ", Journal of American Helicopter Society, Vol. 22, No. 2-3, 1977.

2. Mavris, D. N., Komerath, N. K., and McMahon, H. M., "Prediction of Aerodynamic Rotor-Airframe Interaction in Forward Flight", Journal of the American Helicopter Society, Vol. 34, No. 4, pp. 37-46,1989.

3. Lorber, P. F., and Egolf, T. A., "An Unsteady Helicopter Rotor-Fuselage Aerodynamic Interaction Analysis", Journal of the American Helicopter Society, Vol. 35, No. 3, pp 32-42, 1990.

4. Ruffin, S. M., O' Brien, D., Smith, M. J., Hariharan, N., Lee, J-D, and Sankar, L., "Comparison of Rotor-Airframe Interaction Utilizing Overset and Unstructured Grid Techniques", AIAA 2004-0046, 2004

5. Hariharan, N., and Sankar, L. N., "Unsteady Overset Simulation of Rotor-Airframe Interaction", Journal of Aircraft, Vol. 40, No. 4, pp. 662-674, 2003.

6. Park, Y. M., Nam, H. J., and Kwon, O. J., "Simulation of Unsteady Rotor-Fuselage Aerodynamic Interaction Using Unstructured Adaptive Meshes", Journal of the American Helicopter Society, vol. 51, no. 2, pp. 141-149, 2006.

7. Chaffin, M. S., "A Guide to the Use of the Pressure Disk Rotor Model as Implemented in INS3D-UP", NASA CR-4692, 1995.

8. Rajagopalan, R. G., Rickehl, T. L., and Klimas, P. C., "Aerodynamic Interference of Two Vertical Axis Wind Turbines", AIAA-1988-2534, 1988

9. Rajagopalan, R. G., and Zhang, Z., "Performance and flow field of a ducted propeller", AIAA-1989-2673, 1989

10. Rajagopalan, R. G., and Chin, K. L., "Laminar Flow Analysis of a Rotor in Hover", Journal of the American Helicopter Society, Vol. 36, No. 1, pp. 12-23, 1991

11. Rajagopalan, R. G., and Mathur, S. R., "Three Dimensional Analysis of a Rotor in Forward Flight", Journal of the American Helicopter Society, Vol. 38, No. 3, pp. 14-25, 1993.

12. Zori, L. A. J., and Rajagopalan, R. G., "Navier-Stokes Calculations of Rotor-Airframe Interaction in Forward Flight", Journal of the American Helicopter Society, Vol. 40, No. 2, pp. 56-67, 1995.

13. R. G. Rajagopalan, "A Procedure for Rotor Performance, Flowfield and Interference:A Perspective", AIAA-2000- 0116, 2000

14. Ruith, M. R., "Unstructured, Multiplex Rotor Source Model With Thrust And Moment Trimming - Fluent' s VBM Model", AIAA 2005-5217, 2005.

15. Leishman, J. G., "Principles of Helicopter Aerodynamics", Cambridge University Press, 2006

16. Pitt, D. M., and Peters, D. A., "Theoretical Prediction of Dynamic-Inflow Derivatives", Vertica, Vol. 5, pp. 21-34, 1981

17. Peters, D. A., and He, C. J., "Finite State Induced Flow Models Part Ⅱ: Three-Dimensional Rotor Disk", Journal of Aircraft, Vol. 32, No. 2, pp.323-333, 1995

18. Brand, A. G., McMahon, H. M., and Komerath, N. M., "Surface Pressure Measurements on a Body Subject to Vortex Wake Interaction", AIAA Journal, Vol. 27, No. 5, pp. 569-574, 1989

19. Liou, S. G., Komerath, N. M., and McMahon, H. M., "Velocity Measurements of Airframe Effects on a Rotor in Low-Speed Forward Flight", Journal of Aircraft, Vol. 26, No. 4, pp. 340-348, 1989.

20. CD-adapco Group, 2004, STAR-CD Version 3.20 Methodology.